

The adsorption of 4-*tert*-butylpyridine on the nanocrystalline TiO₂ and Raman spectra of dye-sensitized solar cells in situ

Chengwu Shi^{a,b}, Songyuan Dai^{a,*}, Kongjia Wang^a, Xu Pan^a, Fantai Kong^a, Linhua Hu^a

^a *Institute of Plasma Physics, Chinese Academy of Sciences, P.O. Box 1126, Hefei, Anhui, 230031, PR China*

^b *School of Chemical Engineering, Hefei University of Technology, Hefei, Anhui, 230009, PR China*

Received 25 October 2004; received in revised form 21 December 2004; accepted 4 January 2005

Available online 23 February 2005

Abstract

In this article, we studied the adsorption of 4-*tert*-butylpyridine (TBP) on the nanocrystalline TiO₂ (anatase) powder by Raman, IR and XPS. In Raman spectra, the free TBP and physisorbed TBP showed the totally symmetric ring breathing mode at 996 cm⁻¹ and the vibration of the trigonal symmetry ring stretching mode was too weak to identify, while the coordinated TBP produced the characteristic trigonal symmetry ring stretching mode at 1022 cm⁻¹ and the vibration of the totally symmetric ring breathing mode shifted from 996 to 1007 cm⁻¹. From Raman spectra of dye-sensitized solar cells in situ, the Raman line at 167–169 cm⁻¹ should be assigned to the formation of TBP-I₂ or iodine adsorbed on the dye. Since there were significant differences from 100 to 300 cm⁻¹, we suggested that TBP, besides the adsorption on TiO₂, can also remove iodine adsorbed on the dye to suppress the rate of interfacial electron transfer from the conduction band of TiO₂ to iodine.

© 2005 Elsevier B.V. All rights reserved.

Keywords: 4-*tert*-Butylpyridine; Nanocrystalline TiO₂; Adsorption; Raman spectra; Electrolyte; Dye-sensitized solar cell

1. Introduction

Dye-sensitized solar cells (DSCs) have been extensively studied for their high photoelectric conversion efficiency, their simple assemble technology, and their potential low cost [1–10]. DSCs consist of three main components: a dye-sensitized mesoporous TiO₂ film on a transparent fluorine-doped tin oxide conducting glass as a sensitized photoanode, an electrolyte solution containing triiodide/iodide ions as a redox couple, and a platinized fluorine-doped tin oxide conducting glass as a counter electrode. 4-*tert*-Butylpyridine or *N*-methylbenzimidazole is widely used as additive in electrolytes, owing to their dramatic improvement of the fill factor and the open circuit voltage of DSCs. Since 4-*tert*-butylpyridine is expected to adsorb at the unoccupied dye-absent TiO₂ surface, this effect is supposed to decrease the rate of interfacial electron transfer from the conduction band

of TiO₂ to triiodide [3,11–13]. Moreover, Falaras et al. [14] finds that resonance Raman scattering is a powerful tool to obtain information on the semiconductor, dye, the electrolyte alternatively and the corresponding interfaces in DSCs, and in detail studied the dye chemisorption on nanocrystalline titanium dioxide thin films and the dye–redox couple interactions. By resonance Raman scattering tests, Hagfeldt et al. [15] suggests that long-term stability of DSCs can also be improved because the addition of 4-*tert*-butylpyridine suppresses the loss of the thiocyanato group from the dye and subsequent formation of the I₂·NCS⁻ ion and dye *cis*-bis(iodo)bis(2,2'-bipyridine-4-carboxylic acid,4'-carboxylate)ruthenium(II).

In this article, we report a systematic study of the adsorption of 4-*tert*-butylpyridine on the nanocrystalline TiO₂ (anatase) powder by laser Raman spectrometry, infrared spectrometry and X-ray photoelectron spectroscopy. The Raman scattering in situ was based on the freshly prepared DSCs containing the different electrolytes at the open circuit and short circuit conditions, and the

* Corresponding author. Tel.: +86 551 5591377; fax: +86 551 5591310.
E-mail address: sydai@ipp.ac.cn (S. Dai).

electrochemical behavior of DSCs in dark was involved in this study. In addition, we measured the Raman spectra of the various electrolytes.

2. Experimental

2.1. Materials

Anhydrous lithium iodide, iodine, 4-*tert*-butylpyridine (TBP) and 3-methoxypropionitrile (MePN) were purchased from Fluka, and used as received. 1,2-Dimethyl-3-propylimidazolium iodide (DMPII) was synthesized from 1,2-dimethylimidazole (Aldrich) and propyl iodide (Fluka) [16], its purity was confirmed by 600-MHz ^1H NMR (DMX-600, Bruker, Switzerland).

2.2. DSCs assembly

Briefly, the TiO_2 (anatase) colloidal solution was prepared by hydrolysis of titanium tetraisopropoxide [17]. The surface area of TiO_2 powder was $80 \text{ m}^2/\text{g}$ by BET, the average particle was 13.6 nm by XRD. TiO_2 paste was deposited on the transparent conducting glass sheets (TEC-8, LOF) by using screen-printing technique. The TiO_2 films were sintered in air at 450°C for 30 min to form a nanostructured TiO_2 electrode. The film thickness was $11 \mu\text{m}$, determined by a profilometer (XP-2, AMBIOS Technology Inc., USA). After cooling to 80°C , the films were immersed in a $5.0 \times 10^{-4} \text{ M}$ *cis*-dithiocyanate-*N,N'*-bis-(4-carboxylate-4'-tetrabutylammoniumcarboxylate-2,2'-bipyridine)ruthenium(II) (N719) in anhydrous ethanol solution overnight. The excess of N719 dye in TiO_2 films was rinsed off with anhydrous ethanol. The counter electrode was platinized by spraying H_2PtCl_6 solution to TCO glass and fired in air at 410°C for 20 min. Then, the counter electrode was placed directly on the top of the dye-sensitized TiO_2 film. The gap between the two electrodes was sealed by thermal adhesive films (Surlyn, Dupont). The electrolyte was filled from a hole made on the counter electrode, which was later sealed by a cover glass and thermal adhesive films. The active electrode area of DSCs was 0.16 cm^2 .

2.3. Adsorption and desorption of TBP

TiO_2 powder was prepared by the method of heating TiO_2 paste in air at 450°C for 2 h to remove OH groups of anatase [18]. There were three steps in the preparation of TBP-adsorbed TiO_2 powder. First, TiO_2 (anatase) powder was heated in air at 220°C for 2 h and then cooled to room temperature in a desiccator. Second, the TiO_2 powder absorbed TBP vapor in a closed desiccator at room temperature for 240 h. Finally, the TiO_2 powder that had absorbed TBP vapor was heated in air at 220°C for 1 h to remove the free TBP and physisorbed TBP.

2.4. Measurements

Electrochemical data of DSCs in dark were obtained by linear sweep voltammetry using an electrochemical workstation (CHI660A, CH Instruments Inc., USA). The working electrode was the dye-sensitized TiO_2 film of DSCs. The auxiliary electrode and the reference electrode was the platinized conducting glass of DSCs.

Infrared spectra were measured with a Fourier transform infrared spectrometer (MAGNA-IR 750, Nicolet Instrument Co., USA) at a resolution of 4 cm^{-1} with the mixture of the sample and liquid paraffin coated on a KBr window. Photoelectron spectra of different TiO_2 powder were examined on an X-ray photoelectron spectrometer (ESCALAB MK II, VG., UK) with Mg $\text{K}\alpha$ source. As a reference, the C (1s) signal was fixed at 284.65 eV . Broad survey scans (with a scan step 1.00 eV) were run to identify all elements present in the samples, and then detailed scans (with a scan step 0.05 eV) were recorded on which peak was performed to establish precise elemental peak locations.

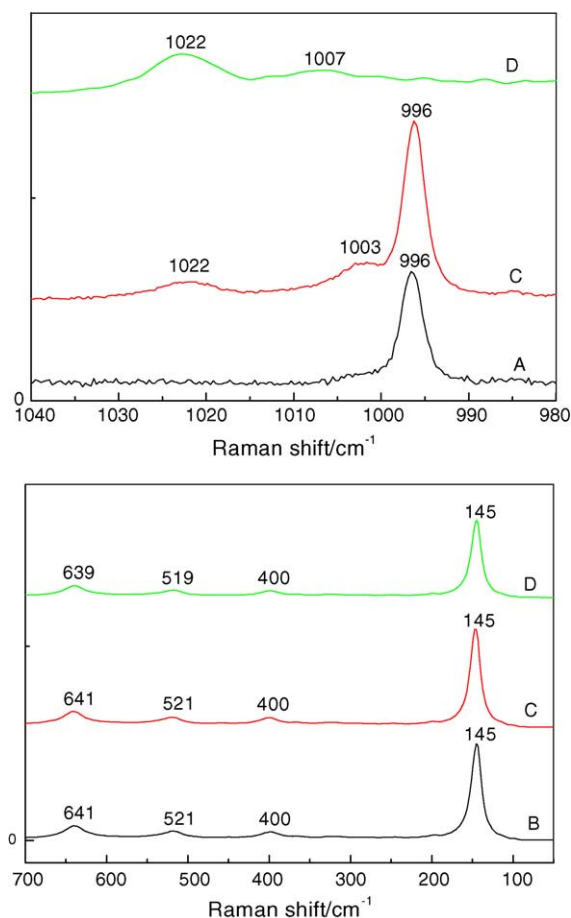


Fig. 1. Raman spectra of sample A: 4-*tert*-butylpyridine liquid; sample B: TiO_2 powder, dried in air at 220°C for 2 h; sample C: sample B, after adsorbing TBP vapor for 240 h at room temperature; sample D: sample C, heated in air at 220°C for 1 h.

Raman spectra of various solutions, TiO₂ powders and DSCs were recorded on a laser micro-Raman spectrometer (LABRAM-HR, JY., France) equipped with a 514 nm argon laser. The laser spot size was approximately 4–5 μm², the power at the sample was estimated to be 1 mW. The Raman spectrometer was calibrated using CCl₄ or a Si single crystal. To measure the Raman spectra of DSCs at open circuit and short circuit in situ, we linked the two electrodes of a DSC with two crocodile clips which were connected with a switch and some wires in advance, and fixed the DSC to the sample platform of the laser micro-Raman spectrometer. At open circuit, we first measured the Raman spectra of the DSC illuminated continuously by 514 nm laser at the different illumination time ($t = 0, 3,$ and 6 min). After 8-min exposure, the DSC was placed to short circuit condition by the switch, and the Raman spectra were measured at the different illumination time ($t = 8, 11,$ and 14 min). The integral calculus time of the DSCs' Raman spectra in situ was 60 s.

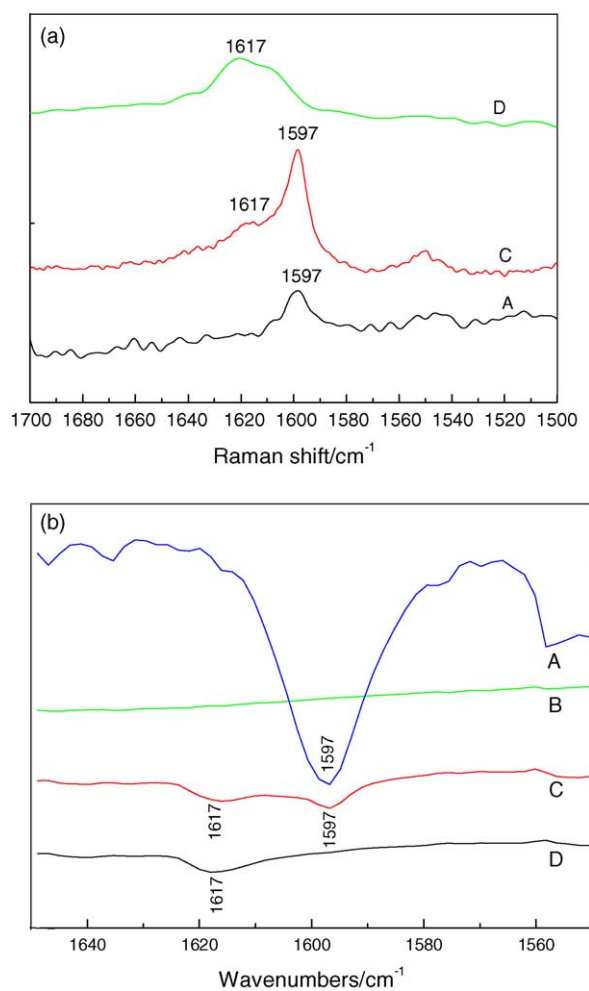


Fig. 2. (a) Raman spectra of samples A, C, and D; (b) infrared spectra of samples A, B, C, and D.

3. Results and discussions

3.1. Adsorption of TBP

Fig. 1 shows the Raman spectra of sample A (TBP, liquid), sample B (TiO₂ powder, dried in air at 220 °C for 2 h), sample C (TiO₂ adsorbed TBP vapor for 240 h at room

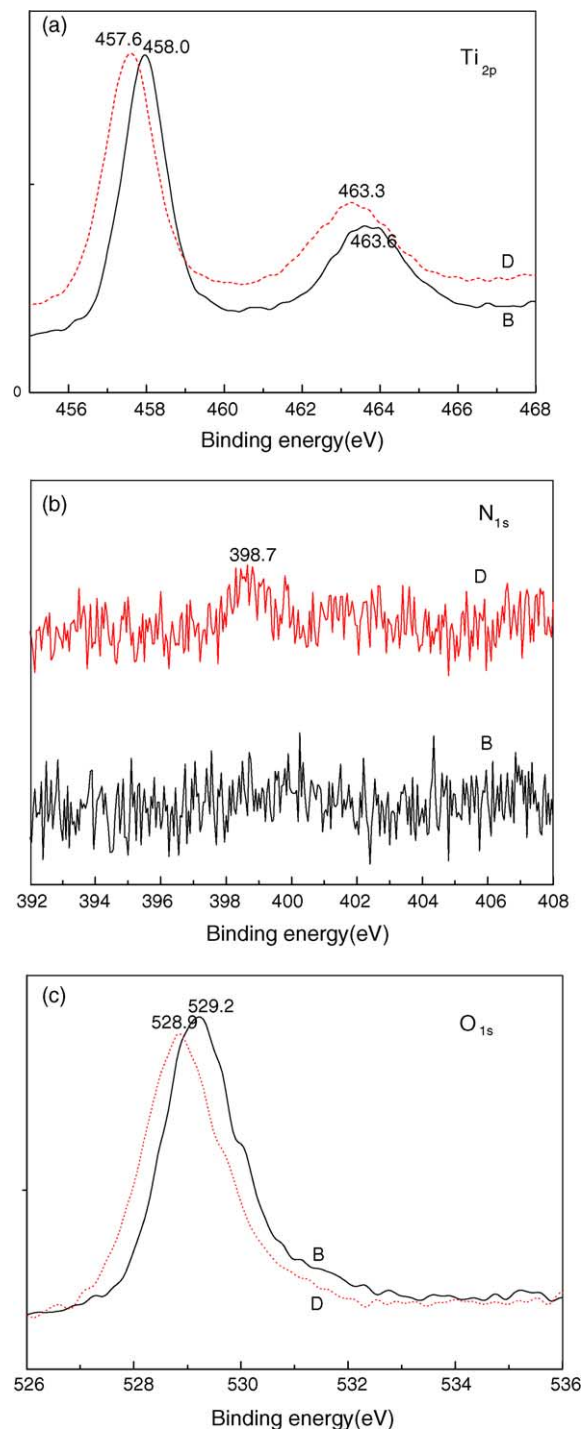


Fig. 3. XPS spectra: the spectral region of Ti_{2p}, N_{1s}, and O_{1s} in samples B and D.

temperature), and sample D (same as sample C, but heated in air at 220 °C for 1 h). Sample C shows the vibrations at 996, 1003, and 1022 cm^{-1} . In sample D, the 996 cm^{-1} bond disappear, and the 1007 and 1022 cm^{-1} bonds are detected. Therefore, the strong bond at 996 cm^{-1} is associated with the totally symmetric ring breathing mode due to the presence of the free TBP and physisorbed TBP, while the vibration of the trigonal symmetry ring stretching mode is too weak to identify. The medium intense bond at 1022 cm^{-1} is associated with the trigonal symmetry ring stretching mode owing to the presence of the coordinated TBP, whereas the vibration of the totally symmetric ring breathing mode shifts from 996 to 1007 cm^{-1} [19–23], and the scattering intensity of 1007 cm^{-1} is weaker than 1022 cm^{-1} . This demonstrates that some titanium atoms on the surface of nanocrystalline TiO_2 powder are incompletely coordinated, and can bind TBP molecules by forming $\text{Ti} \leftarrow \text{N}$ bonds. In other words, the coordinated TBP contributes to the characteristic trigonal symmetry ring

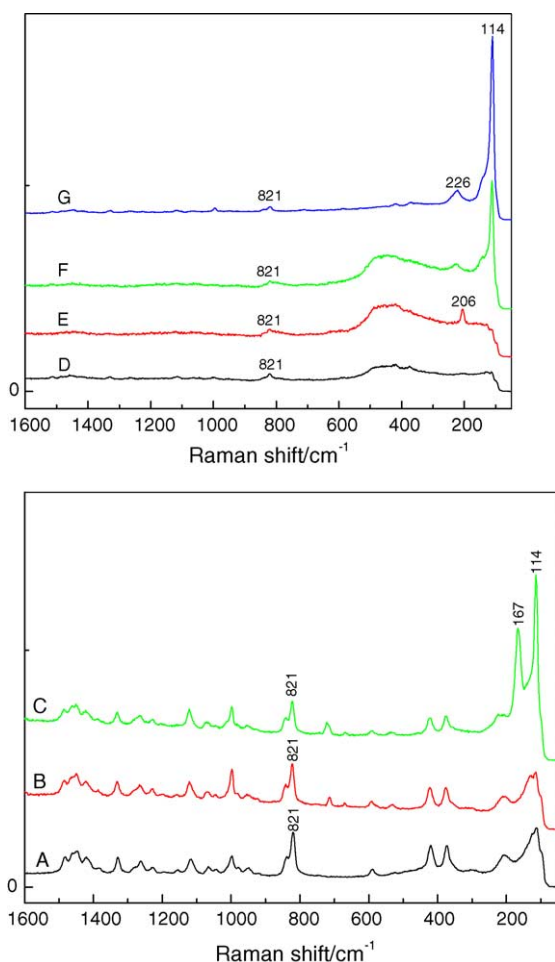


Fig. 4. Raman spectra from the solutions of A (3-methoxypropionitrile liquid), B (0.50 M TBP, in MePN), C (0.50 M TBP, 0.10 M I_2 , in MePN), D (0.50 M DMPII, in MePN), E (0.10 M I_2 , in MePN), F (0.50 M DMPII, 0.10 M I_2 , in MePN), and G (0.50 M DMPII, 0.10 M I_2 , 0.50 M TBP, in MePN).

stretching mode at 1022 cm^{-1} . The characteristic Raman vibrations of sample B are similar to samples C and D, and there are no apparent changes after sample B adsorbs TBP. The Raman lines at 145, 400, 521, and 641 cm^{-1} of sample B can be assigned to the E_g , B_{1g} , A_{1g} or B_{2g} and E_g modes of the anatase phase, respectively. The result agrees with XRD, which also indicates that the TiO_2 powders are anatase phase.

Fig. 2 presents Raman spectra (samples A, C, and D) and infrared spectra (samples A, B, C, and D). Similar phenomena are observed in the two spectra. The coordinated TBP gives 1617 cm^{-1} bond of the ring stretching vibration, which obviously shifts 20 cm^{-1} , relative to 1597 cm^{-1} bond of the free TBP and physisorbed TBP [24].

Fig. 3 shows X-ray photoelectron spectra of samples B and D (including the peaks of Ti_{2p} , N_{1s} and O_{1s}). Comparing with the binding energy (458.0 eV) of TiO_2 , the full width at half-maximum (FWHM) of this 457.6 eV peak broaden out in sample D, which corresponds with the forming of $\text{Ti} \leftarrow \text{N}$ bonds. There is no apparent difference of the O_{1s} binding energy between samples B and D. The XPS result also indicates that the TBP content is low in sample D and the chemical stoichiometry of Ti to N is about 12:1 from the rate of their intensity.

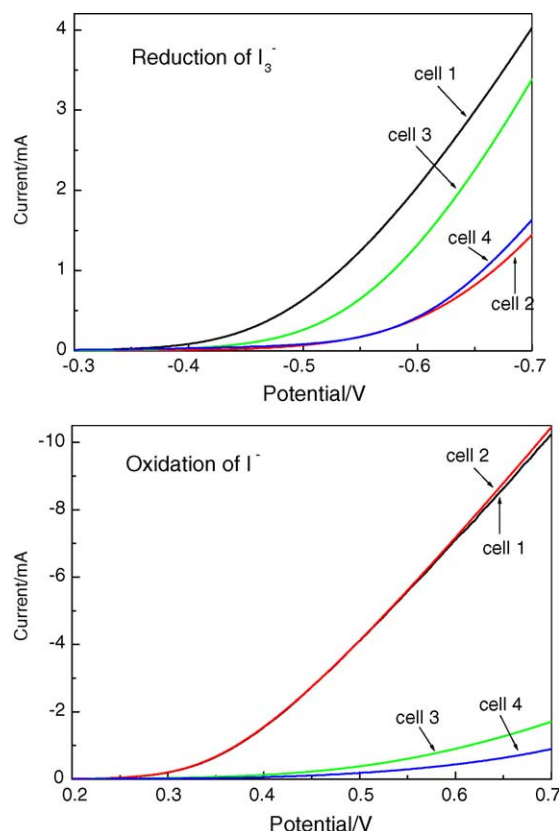


Fig. 5. Linear sweep voltammograms for DSCs. Cell 1: N719, TBP (0.00 M); cell 2: N719, TBP (0.30 M); cell 3: no dye, TBP (0.00 M); cell 4: no dye, TBP (0.30 M). The other components of the electrolyte are the same (DMPII 0.66 M, LiI 0.11 M, I_2 0.10 M, in MePN).

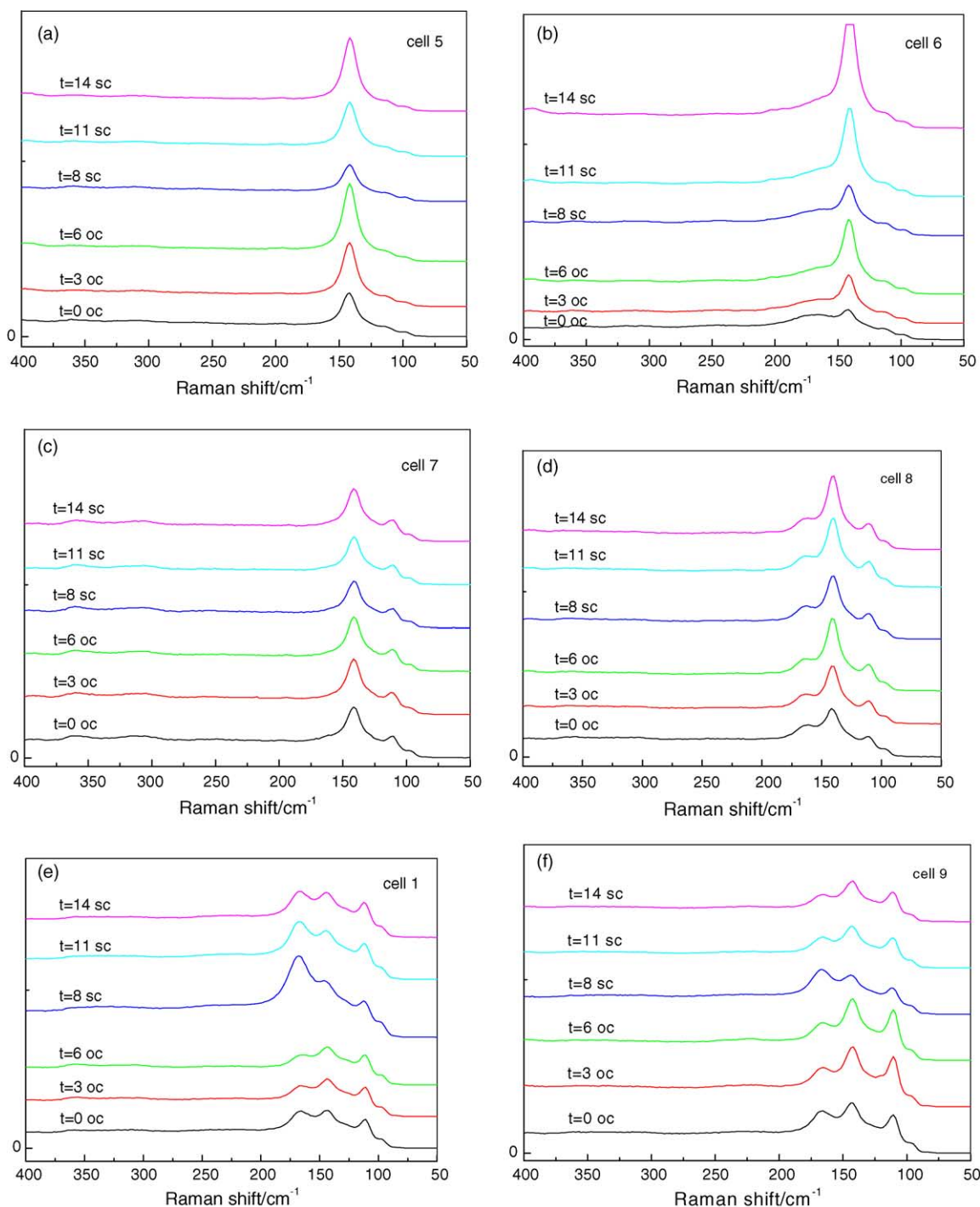


Fig. 6. Raman spectra in situ for DSCs. Cell 5: MePN; cell 6: 0.10 M I_2 , in MePN; cell 7: 0.50 M DMPII, in MePN; cell 8: 0.10 M I_2 , 0.50 M TBP, in MePN; cell 1: 0.00 M TBP; cell 9: 0.51 M TBP. For cells 1 and 9, the other components of the electrolyte are the same (0.66 M DMPII, 0.11 M LiI, 0.10 M I_2 , in MePN). Dye: N719.

From the above, it is demonstrated that TBP can be chemisorbed on the surface of nanocrystalline TiO_2 by the forming of $Ti \leftarrow N$ bonds. Comparing Raman, IR and XPS, Raman is particularly useful for examining the forming of $Ti \leftarrow N$ bonds by introducing the tertiary butyl into the para position of N atom of pyridine.

3.2. Raman scattering of I_3^- and $I_2 \cdot TBP$ from solutions

Fig. 4 shows the Raman spectra from MePN and some solutions. According to these Raman spectra, we conclude that the Raman lines at 114 and 226 cm^{-1} are from the anions I_3^- , and the Raman line at 206 cm^{-1} is due to the

formation of a $I_2 \cdot \text{MePN}$ solvent complex. This agrees with the references [15,25]. It should be noted that the Raman line at 167 cm^{-1} is assigned to the formation of a stable $I_2 \cdot \text{TBP}$ molecular complex. Comparing with the intensity of the Raman lines at 114 and 167 cm^{-1} of C and G in Fig. 4, we suggest that the anions I_3^- is more stable than $I_2 \cdot \text{TBP}$. In other words, $I_2 \cdot \text{TBP}$ can react with I^- ions to give free TBP and the anions I_3^- .

3.3. Influence of dye and TBP on I_3^-/I^- redox reaction on the TiO_2 electrode

Fig. 5 shows the linear sweep voltammograms of the various DSCs in dark. By comparison of cells 1 and 3, it is observed that the dye can improve the reduction of I_3^- and the oxidation of I^- without TBP in the electrolyte. Comparing cell 1 with cell 2, we conclude that TBP can suppress the reduction of I_3^- , and the same conclusion can be obtained from comparison of cells 3 and 4. On cells 1 and 2, TBP has little influence on the oxidation of I^- on the dye-sensitized TiO_2 film. By cells 3 and 4, TBP has a little influence on the oxidation of I^- because of chemisorption of TBP on the TiO_2 film without dye-sensitization. Thus, it can be concluded that the dye plays an important role in the redox reactions of I_3^-/I^- , which should be the result of interaction between I^- or I_3^- and the sulfur atom of the thiocyanate ligands of N719 [15], and TBP suppresses the reduction of I_3^- on the TiO_2 electrode.

3.4. Raman spectra of DSCs in situ

To know the effect of TBP on DSCs, we also measured the Raman spectra of DSCs in situ at open circuit and short circuit. Fig. 6 shows that the Raman line at 144 cm^{-1} appears in cell 5; 144 and 169 cm^{-1} in cell 6; 112 and 144 cm^{-1} in cell 7; 112 , 144 and 169 cm^{-1} in the cells 8, 1, and 9. Obviously, the Raman line at 112 cm^{-1} is from I_3^- , and 144 cm^{-1} is from TiO_2 , which are in accordance with the literature [15,25]. The assignment of Raman line at 169 cm^{-1} is complex and needs more discussions. No apparent differences from 300 to 1600 cm^{-1} can be seen in these Raman spectra of DSCs in situ at the open-circuit and short circuit conditions. However, there are significant differences from 100 to 300 cm^{-1} .

Table 1 displays the intensity ratio evolution of the Raman lines at 112 and 169 cm^{-1} with time. In cells 1 and 9, the

169 cm^{-1} intensity of $t = 8$ min at short circuit is stronger than that of $t = 6$ min at open circuit. With the decrease of the electron occupancy in conducting band of TiO_2 film at short circuit ($t = 8$ min), more I^- is absorbed on the dye, and subsequently the iodine adsorbed on the dye is produced. Thus, we suggest that the Raman line at 169 cm^{-1} should be assigned to the formation of $\text{TBP} \cdot I_2$, or iodine adsorbed on the dye. Falaras et al. also discuss the assignment of the band and suggests that the triiodide is attached to the dye by electrostatic forces, $[\text{D}^+]\text{I}_3^-$, and the 169 cm^{-1} band of DSCs should be not assigned to the formation of a complex between triiodide and thiocyanate [14,15]. This is in accordance with our result. But because polyiodide anions and interactions of dye–redox couple are complex, it should be further researched whether the iodine adsorbed on the dye is $[\text{D}^+]\text{I}_3^-$. In cell 1 (without TBP), the intensity of 169 cm^{-1} changes from 1.0 to 11.7 whereas in cell 9 (0.51 M TBP) from 0.6 to 3.2 , we conclude that TBP can remove the adsorption of iodine on the dye, which agrees with the result of linear sweep voltammetry. The 144 cm^{-1} intensity of cell 5 at short circuit ($t = 8$ min) is weaker than that of $t = 6$ min at open circuit, this result may be caused by the decrease of the electron occupancy in conducting band of TiO_2 film.

4. Conclusions

Adsorption of TBP on the nanocrystalline TiO_2 (anatase) powder was investigated by Raman, IR and XPS. It was demonstrated that some incompletely coordinated titanium atoms on the surface of nanocrystalline TiO_2 powder can bind TBP molecules by forming $\text{Ti} \leftarrow \text{N}$ bonds. The free TBP and physisorbed TBP shows the totally symmetric ring breathing mode at 996 cm^{-1} , and the vibration of the trigonal symmetry ring stretching mode is too weak to identify, while the coordinated TBP produce the characteristic trigonal symmetry ring stretching mode at 1022 cm^{-1} and the vibration of the totally symmetric ring breathing mode shift from 996 to 1007 cm^{-1} .

In this article, we suggest that the Raman line at 167 – 169 cm^{-1} should be assigned to the formation of $\text{TBP} \cdot I_2$ or iodine adsorbed on the dye. No apparent differences from 300 to 1600 cm^{-1} can be seen in these Raman spectra of DSCs in situ at the open-circuit and short circuit conditions. However, there are significant differences from 100 to 300 cm^{-1} . We conclude that TBP, besides the adsorption on TiO_2 , can also remove iodine adsorbed on the dye to suppress the rate of interfacial electron transfer from the conduction band of TiO_2 to iodine.

Acknowledgment

This work is financially supported by the National Key Project of China for Basic Research under Grant No. G2000028200.

Table 1

Intensity ratio evolution of the Raman lines at 112 and 169 cm^{-1} with time

$I(112 \text{ cm}^{-1})/I(169 \text{ cm}^{-1})$	Cell 1	Cell 9
$t = 0$ min, open circuit	1:1.8	1:1.3
$t = 3$ min, open circuit	1:1.2	1:0.7
$t = 6$ min, open circuit	1:1.0	1:0.6
$t = 8$ min, short circuit	1:11.7	1:3.2
$t = 11$ min, short circuit	1:3.2	1:1.0
$t = 14$ min, short circuit	1:1.9	1:0.8

Appendix A. Supplementary data

Supplementary data associated with this article can be found, in the online version, at [doi:10.1016/j.vibspec.2005.01.002](https://doi.org/10.1016/j.vibspec.2005.01.002).

References

- [1] B. O'Regan, M. Grätzel, *Nature* 353 (1991) 737.
- [2] A. Hagfeldt, M. Grätzel, *Chem. Rev.* 95 (1995) 49.
- [3] M.K. Nazeeruddin, A. Kay, I. Rodicio, R. Humphry-Baker, E. Müller, P. Liska, N. Vlachopoulos, M. Grätzel, *J. Am. Chem. Soc.* 115 (1993) 6382.
- [4] M.K. Nazeeruddin, P. Péchy, T. Renouard, S.M. Zakeeruddin, R. Humphry-Baker, P. Comte, P. Liska, L. Cevey, E. Costa, V. Shklover, L. Spiccia, G.B. Deacon, C.A. Bignozzi, M. Grätzel, *J. Am. Chem. Soc.* 123 (2001) 1613.
- [5] S. Kambe, S. Nakade, T. Kitamura, Y. Wada, S. Yanagida, *J. Phys. Chem. B* 106 (2002) 2967.
- [6] P. Wang, S.M. Zakeeruddin, P. Comte, I. Exnar, M. Grätzel, *J. Am. Chem. Soc.* 125 (2003) 1166.
- [7] W. Kubo, S. Kambe, S. Nakade, T. Kitamura, K. Hanabusa, Y. Wada, S. Yanagida, *J. Phys. Chem. B* 107 (2003) 4374.
- [8] U. Bach, D. Lupo, P. Comte, J.E. Moser, F. Weissörtel, J. Salbeck, H. Spreitzer, M. Grätzel, *Nature* 395 (1998) 583.
- [9] S.A. Sapp, C.M. Elliott, C. Contado, S. Caramori, C.A. Bignozzi, *J. Am. Chem. Soc.* 124 (2002) 11215.
- [10] S.-Y. Dai, K.-J. Wang, *Chin. Phys. Lett.* 20 (2003) 953.
- [11] S.A. Haque, Y. Tachibana, R.L. Willis, J.E. Moser, M. Grätzel, D.R. Klug, J.R. Durrant, *J. Phys. Chem. B* 104 (2000) 538.
- [12] H. Lindström, H. Rensmo, S. Södergren, A. Solbrand, S.E. Lindquist, *J. Phys. Chem.* 100 (1996) 3084.
- [13] S.Y. Huang, G. Schlichthörl, A.J. Nozik, M. Grätzel, A.J. Frank, *J. Phys. Chem. B* 101 (1997) 2576.
- [14] P. Falaras, T. Stergiopoulos, M.C. Bernard, A.H.L. Goff, *Coord. Chem. Rev.* 248 (2004) 1407.
- [15] A. Hagfeldt, H. Greijer, J. Lindgren, *J. Phys. Chem. B* 105 (2001) 6314.
- [16] P. Bonhôte, A.P. Dias, N. Papageorgiou, K. Kalyanasundaram, M. Grätzel, *Inorg. Chem.* 35 (1996) 1168.
- [17] L. Hu, S. Dai, K. Wang, *Acta Phys. Sin.* 52 (2003) 2135 (in Chinese).
- [18] M. Primet, P. Pichat, M.V. Mathieu, *J. Phys. Chem.* 75 (1971) 1216.
- [19] F.R. Dollish, W.G. Fateley, F.F. Bentley, *Characteristic Raman Frequencies of Organic Compounds*, John Wiley, 1974.
- [20] S.F. Simpson, J.M. Harris, *J. Phys. Chem.* 94 (1990) 4649.
- [21] R.O. Kagel, *J. Phys. Chem.* 74 (1970) 4518.
- [22] P.J. Hendra, I.D.M. Turner, E.J. Loader, M. Stacey, *J. Phys. Chem.* 78 (1974) 300.
- [23] G.L. Schrader, C.P. Cheng, *J. Phys. Chem.* 87 (1983) 3675.
- [24] M. Primet, P. Pichat, M.V. Mathieu, *J. Phys. Chem.* 75 (1971) 1221.
- [25] T. Tassaing, M. Besnard, *J. Phys. Chem. A* 101 (1997) 2803.